Journal of Colloid and Interface Science 255 (2002) 363-374

Correlations between Surface and Interface Energies with Respect to Crystal Nucleation

BERNARD VINET[1*], LENA MAGNUSSON[2], HASSE FREDRIKSSON[2], AND PIERRE JEAN DESRÉ[3]

1 Commissariat à l'Énergie Atomique, Direction de la Recherche Technologique, Département des Technologies pour les Énergies Nouvelles, 17 rue des Martyrs, 38054 Grenoble, Cédex 9, France
2 Royal Institute of Technology, Department of Casting of Metals, Brinell väg, 100 44 Stockholm, Sweden
3 Institut National Polytechnique de Grenoble, Laboratoire de Thermodynamique et Physico-chimie Métallurgiques, 38402 Saint-Martin d'Hères, France

The energetic chemical and structural properties of interfaces between solid and liquid metals are of great interest in numerous applications. However, solid-liquid interfacial energy of metals are often determined by nucleation experiments, requiring particular attention to the measurements so obtained. The purpose of this paper is to conduct an analysis of the level of liquid undercooling of *3d*-, *4d*- and *5d*- transition metals, as well as of other common undercooled elements, through a critical survey of thermophysical data and experimental results. As already pointed out for the liquid-vapour surface energy σ_{LV}, the solid-liquid interface energy σ_{LS} determined from the maximum amount of liquid undercooling is well connected to the position of the element in the periodic table leading to individualize each behaviour, including the size of the critical nucleus. The β ratio of σ_{LS}/σ_{LV} is demonstrated to be an interesting dimensionless number to classify the elements into distinctive groups. No significant unexplained anomaly is identified, except for Co, making believe that Turnbull's classical theory furnishes a robust support to describe the crystal nucleation in pure elements.

Key words: Crystal nucleation, liquid undercooling, transition metals, liquid-vapour surface energy, solid-liquid interface energy, drop-tube experiments, container-less processing.

I. INTRODUCTION

A finite amount of liquid undercooling is required to initiate solidification. An undercooled melt is in a metastable state and nucleation is the first step of the phase transition, selecting the primary phase of growth. The understanding of nucleation is therefore of major importance for a better control of solidification. The physical origin of liquid metastability is well explained on the basis of Gibbs work, but this work provides no answer to the question of what is the undercooling limit in temperature. It seems to be difficult to develop a quantitative theory of nucleation and to verify the occurrence of homogeneous nucleation which identifies with this limit (in opposition to heterogenous nucleation due to catalytic effects of foreign particles). Since the phenomenon of liquid undercooling translates the construction of a viable solid-liquid interface, the objective is finally in measuring and modelling of surface energies. Apart from nucleation and crystal growth from the melt, the energetic, chemical and structural properties of interfaces between solid and liquid metals are of great interest in wetting phenomena, liquid phase sintering and embrittlement of solids by liquids metals (1). However, most published values of solid-liquid interfacial energy of metals are determined by nucleation experiments, requiring particular attention to the measurements so obtained.

From an experimental point of view, the state of liquid undercooling was discovered by Fahrenheit on water when working on the thermometer (2). Later on, Cavendish (3) found this phenomenon in Hg protected by nitritic acid and fats. In the same way, Despretz (4) undercooled water down to - 20°C and

* To whom correspondence should be addressed at CEA, DTEN, Laboratoire Élaboration Solidification et Assemblage, 17 rue des Martyrs, 38054 Grenoble, Cédex 9, France
Tel : (33) 4 38 78 40 99, Fax : (33) 4 38 78 51 17; e-mail : vinet@chartreuse.cea.fr

noticed that solidification proceeded rapidly, causing the glass vessel destruction. Interesting observations were also realized by Gernez (5) and Van Riemsdyk (6), *e.g.* the detrimental effect on undercooling of discontinuous cooling, isomorphous solid particles, and stirring. In 1908, Mendenhall and Ingersoll (7) noted "several rather curious phenomena" when heating minute particles of various metals placed upon the surface of a Nernst glower, whose temperature could be controlled with a suitable rheostat and examined with a microscope of low power. As a matter of fact they obtained very large undercoolings, *e.g.* 375 K on Pt. Still later, Vonnegut (8) demonstrated that dividing the melt into small particles could isolate heterogeneous nucleation sites. These last two works established the dispersion techniques as the suitable way to investigate the undercooling behaviour of numerous pure metals and semi metals. These techniques were successfully improved and extended by Turnbull (9), Rasmussen (10), Perepezko (11), Bosio (12) and co-workers. In the advent of container-less processing methods, deep undercoolings unseen previously on bulk liquids were achieved (13). Recently, high drop-tube facilities (14,15) allowed investigating refractory transition metals up to W.

From a theoretical point of view, Gibbs (16) proposed in 1873, a thermodynamic analysis on phase stability leading him to distinguish between localised and delocalised perturbations and/or fluctuations in the melt (concerning respectively a fraction of phase particles and the entire phase). In the case of classical nucleation, metastability corresponds to the situation where a critical size exists within a localized fluctuation beyond which growth occurs. The capillary formalism attached to the concept of critical nucleus simply allows to consider the Gibbs free-energy difference ΔG of a spherical nucleus in the melt as the sum of a volume and an interface term,

$$\Delta G = \frac{4}{3}\pi r^3 \Delta G_V + 4\pi r^2 \sigma_{LS} \quad , \qquad [1]$$

where r is the radius, σ_{LS} is the solid-liquid interfacial energy (in $J.m^{-2}$), and ΔG_V the negative free enthalpy change in forming a unit of volume of solid from the liquid (in $J.m^{-3}$). ΔG is shown to exhibit a maximum as a function of r, which forms an activation barrier of height ΔG^* at a critical nucleus r^*:

$$\Delta G^* = \frac{16}{3}\pi \frac{\sigma_{LS}^3}{\Delta G_V^2} \qquad \text{and} \qquad r^* = -2\frac{\sigma_{LS}}{\Delta G_V} \quad . \qquad [2a,b]$$

In 1926, Volmer and Weber (17) used this formalism to find the nucleation rate from a supersaturated condensed vapour. They identified the fluctuations to (liquid) embryos, from where they calculated the nuclei distribution assuming that the nucleation rate is proportional to the critical nuclei population. An improved treatment was proposed by Becker and Döring (18) considering that embryos of critical size are formed by a sequence of bimolecular processes involving vapour molecules and subcritical embryos some of which are dissolved. The theory for the rate of homogeneous nucleation in condensed systems was finally proposed by Turnbull and Fisher (19,20). This theory provides a possibility to determine σ_{LS} from experiments. They derived the following expression for the frequency J of the formation of crystal nuclei per unit volume of an undercooled liquid (i.e. the nucleation rate)

$$J = K_V \exp\left(-\frac{\Delta G^*}{k_B T}\right) \quad , \qquad [3]$$

where k_B is the Boltzmann constant and T is the temperature. Limited across the phase boundary, K_V is estimated to be close $10^{39\pm1}$ $s^{-1}.m^{-3}$. Since reaching 10^{35} $s^{-1}.m^{-3}$ at the very most for heterogeneous nucleation, the determination of K_V is considered the clearest way to distinguish properly between homogeneous and heterogeneous processes. This can be undertaken by studying the effect of sample size on nucleation or, according to Skripov (21), by analysing the full width at half maximum of the distribution of nucleation events. The first method, practiced by Turnbull (22) on liquid Hg droplets, requires a significant variation of the sample volume, which in turn introduces different experimental conditions. The latter statistical method implies an accurate resolution of the temperature, as the critical undercooling can be quite narrowly defined. Finally, the difficulty in measuring K_V is such that it is often not possible to ascertain homogeneous nucleation in practice.

Keeping in mind that the limit to crystal nucleation is an intrinsic property of the element under consideration (23), the explanation of the attainable amount of liquid undercooling for each element

should be regarded as an ultimate objective in this domain. In such a way, the study of refractory metals appears of major importance from a methodological point of view for three reasons. First, undercooling experiments have essentially dealt with elements ranging between Hg and Fe in melting temperature, thus by considering in a common approach elements characterized by very different physical and chemical properties. The *3d*-series is characterized by the occurrence of magnetic effects as well as by the numerous allotropic transformations of Mn. The undercooled non transition elements like metals (Al, Pb, In, Ga, Sn), semimetals (Bi, Sb) or semiconductors (Si, Ge) display a large variety of crystallographic structures. On the contrary, *4d*- and *5d*- transition elements (from group IVB to group IIB) offer a remarkable succession of h.c.p., b.c.c., h.c.p. and f.c.c. structures. Second, statistical analysis according to Skripov (21) has given evidence for a homogeneous nucleation process in several refractory metals (24,25), thus offering propitious conditions to discuss the limit to crystal nucleation, at least in the framework of the classical theory of nucleation. Third, an interesting agreement has been noticed (24) between experimental solid-liquid interfacial energies and calculated values from the application of the semi-empirical Skapski correlation (26), where σ_{LS} is expressed as a function of the liquid-vapour surface energy σ_{LV} of the metal at the melting temperature, already correlated to selected physical properties by Allen (27).

The purpose of the paper is to conduct a first analysis of the level of undercooling (the *undercoolability*) of *3d*-, *4d*- and *5d*- transition metals through the research of correlations between σ_{LS} and σ_{LV} values and corresponding dimensionless numbers with respect to the position in the periodic table. This analysis is further extended to the case of other common undercooled elements. The study includes a critical survey of used thermophysical data and experimental results, especially of undercooling amounts leading to σ_{LS} values and liquid-vapour surface energy measurements (see Table 1). Key experiments still useful to clarify the situation on pure elements are suggested in this contribution.

II. COMMENTS ON THE LIMIT TO CRYSTAL NUCLEATION

Let us denote $\Delta T = T_m - T_n$ the amount of undercooling and $\theta = \Delta T/T_m$ the normalized amount of undercooling (T_m is the melting temperature and T_n is the nucleation temperature). Turnbull and Cech (9) remarked that the ΔT values obtained by Mendenhall and Ingersoll (7) are roughly proportional to T_m and established that θ is a constant (0.18 ± 0.02) based on new experiments. The systematic use of a scaling ΔT against T_m allows comparisons between experiments but promotes the speculation of a defined, relatively unique, θ limit for metals. Nonetheless, if we consider the two basic hypotheses made on J (the critical nucleus is unique, *i.e.* $JVt = 1$, where V is the sample volume and t is the time to nucleation) and K_V (10^{39} $s^{-1}.m^{-3}$ for homogeneous nucleation), the relevant term in the exponential [3] is a constant for a given experimental configuration, our choice is then to define the dimensionless number K_V^*,

$$JVt = K_V Vt \exp\left(-\frac{\Delta G^*}{k_B T}\right) \Rightarrow K_V^* \exp\left(-\frac{\Delta G^*}{k_B T}\right) = 1 \quad . \qquad [4]$$

K_V^* is typically 3 x 10^{31} for bulk droplets considered by container-less processing (drop-tube facility, electromagnetic levitation) or 2 x 10^{27} for tiny particles prepared by the dispersion technique. By assuming the classical approximation for ΔG_V of pure melts as the product of the entropy of fusion ΔS_m and ΔT (28), the nucleation barrier can be rewritten using two dimensionless numbers, the normalized amount of undercooling θ and C_n (24):

$$\mathrm{Log}K_V^* = \frac{\Delta G^*}{k_B T} = \frac{C_n}{\theta^2(1-\theta)} \quad , \quad \text{where} \quad C_n = \frac{16}{3}\pi \frac{V_m^2 \sigma_{LS}^3}{k_B T_m^3 \Delta S_m^2} \quad . \qquad [5a,b]$$

V_m is the molar volume ($V_m = M/\rho_{Liq}$, where M is the molar mass and ρ_{Liq} the liquid density) and ΔS_m is the entropy of fusion (in $J.K^{-1}.mol^{-1}$). The graphic interpretation for homogeneous nucleation using the θ - C_n scaling (Fig.1) shows that the absolute limit is an intrinsic property of the material as long as no relation is introduced between the thermophysical properties appearing in C_n.

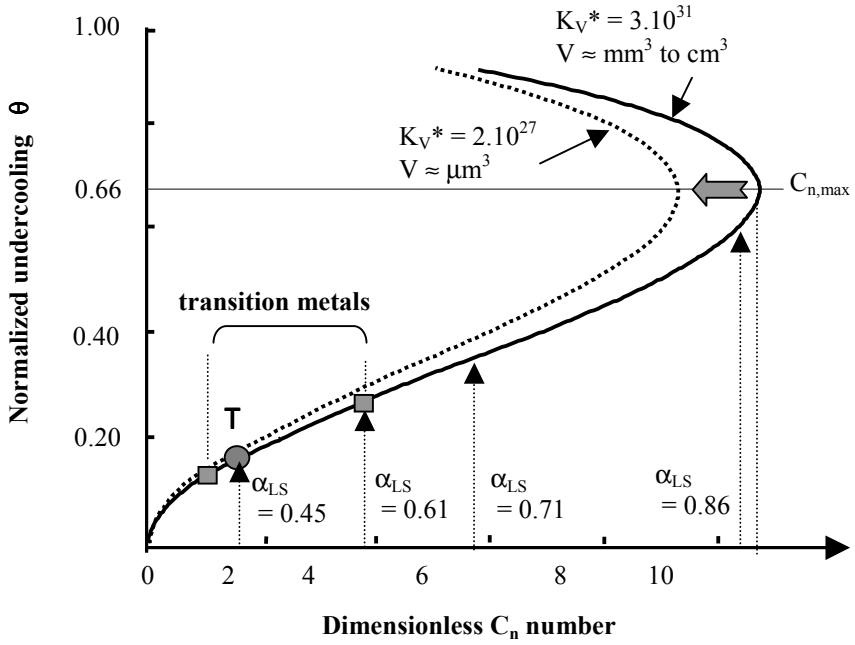

Fig. 1. Graphic representation for homogeneous nucleation in the C_n - θ scaling, arrows identify normalized amounts of undercooling corresponding to different theoretical α_{LS} (for ΔS_m = 8 J.K^{-1}.mol^{-1}), ■ experimental range for transition metals, (T) Turnbull's initial result.

If J increases with θ and reaches a maximum for θ = 2/3 independently of σ_{LS} and ΔS_m values (29), this maximum is clearly an ultimate limit for liquid undercooling, but not a universal limit. C_n can also be expressed versus the dimensionless solid-liquid interfacial energy α_{LS}:

$$C_n = \frac{16}{3}\pi\frac{\Delta S_m}{R}\alpha_{LS}^3 \quad \text{, where} \quad \alpha_{LS} = \frac{(NV_m^2)^{1/3}}{\Delta S_m T_m}\sigma_{LS} = \frac{(NV_m^2)^{1/3}}{\Delta H_m}\sigma_{LS} \qquad [6ab]$$

R is the universal gas constant and *N* is the Avogadro number. ΔH_m is the enthalpy of fusion (in J.mol^{-1}). Assuming that ΔS_m is typically 8 J.K^{-1}.mol^{-1}, Turnbull's initial result ($\theta \approx 0.18$) corresponds to $\alpha_{LS} = 0.45$. Through an actualisation of data (see Table 1), the entropy of fusion of the common undercooled elements is roughly constant for twenty one of them leading to an average value of 9.30 ± 0.35 J.K^{-1}.mol^{-1} as shown in Fig.2. In comparison, slightly lower and higher values are respectively found for a group of seven elements (≈ 7.70 ± 0.35 J.K^{-1}.mol^{-1}), that includes Fe, and for Al, W and Sn. No typical value can be found for Ga, Bi, Sb, Te, Se, Si and Ge.

For large normalized amounts of undercooling (θ > 0.3), the behaviour of the entropy of fusion must be described via a more complex formulation, involving the discontinuity of specific heat between liquid and solid. This is obviously not the case when dealing with pure transition metals (θ < 0.3), so that the classical Turnbull's expression of ΔG_V can readily be applied. In the particular case of Ga, the undercooling is large enough (θ ≈ 0.50) by using the dispersion technique (30) to occur very near to the nose of the θ - C_n curve. Since the maximum value for C_n (i.e. for θ = 2/3) diminishes with K_V^*, the scaling supports the possibility for extremely small Ga droplets, through favourable characteristic times, to stay liquid (*i.e.* to bypass the nose) at the temperature of liquid nitrogen as realized by Koverda et al (31). As a last remark, undercooling experiments are quite systematically performed by continuous cooling of the melt until nucleation. Consequently J is a function of both temperature and time. Nevertheless, according to Zeldovich's approach (32), the kinetic situations characterized by cooling rates lower than a few hundred of K.s^{-1} are far from the extreme kinetic conditions that could influence undercooling (> 10^4 K.s^{-1}). The growth of pure metals from highly undercooled melts is so rapid that nucleation phenomenon and observation of the phase transition at a macroscopic scale through recalescence manifestation (detected by optical pyrometry or using thermocouples) are almost simultaneous.

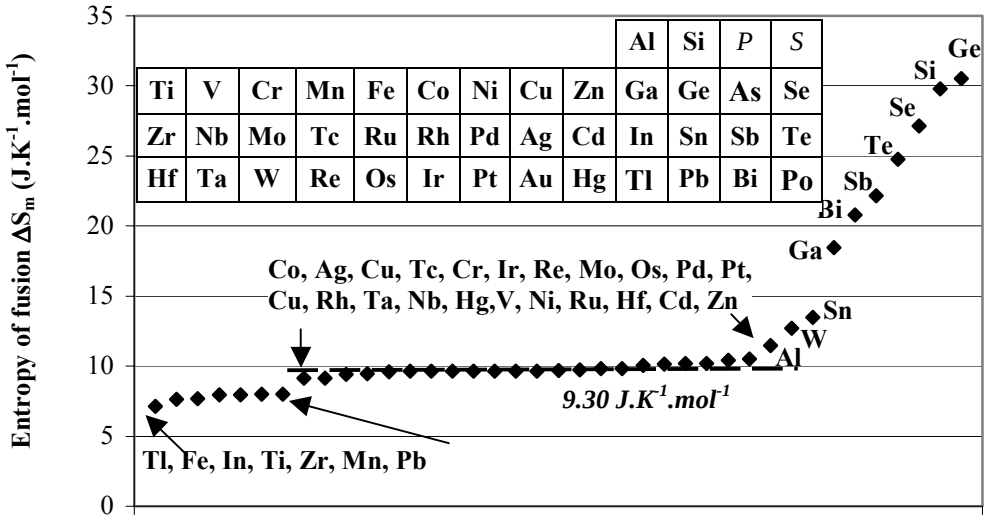

Fig.2. Entropy of fusion of the common undercooled elements (increasing values); detail of the periodic chart of the elements.

The classical theory of nucleation does not allow to a priori predict liquid undercooling and consequently σ_{LS} (or α_{LS}). Different techniques analysed in detail by Howe (33) have been developed to examine the atomic structure and behaviour of the solid-liquid interface: (*i*) analytical or computer-built versions of the Bernal model, which construct hard-sphere models of the interface according to certain packing rules, (*ii*) Monte-Carlo simulations, which utilize the interatomic potential of the atoms and allow an ensemble of atoms to evolve to thermodynamic equilibrium through a series of probabilistic jumps, and (*iii*) molecular dynamics simulations, where the atoms are allowed to move according to the laws of Newtonian mechanics. Recent theoretical developments of crystal nucleation have also been critically reviewed by Gránásy (34) with the emphasis placed on modelling the properties of small clusters. The Spaepen's analysis (35) is the first major attempt to solve the structure of a solid-liquid interface. In this model, the translational order disappears in the first liquid side layer while the order perpendicular to the interface decreases much less. Consequently, the interface is characterized by a very small density deficit, in opposition with models based upon the assumption that the liquid disordered state is directly adjacent to the interface, as proposed for instance by Skapski (26). Through Spaepen's analysis, the α_{LS} values are 0.86 for f.c.c. and h.c.p. and 0.71 for b.c.c. (36,37). Molecular dynamics simulations using various Lennard-Jones potentials yielded α_{LS} values of 0.32 (38) and 0.36 (39). Recently, Iwamatsu (40,41) developed a unified Landau-Ginzburg model derived from microscopic density functional theory that fits well again with the value of $\theta \approx 0.18$ (by considering a prefactor that is orders of magnitude higher than the classical one is assumed). Finally, Davidchack and Laird (42) reported a direct calculation by molecular-dynamics computer simulation of the crystal/melt interfacial free energy. α_{LS} is found to be of 0.51 with a slightly anisotropic effect depending on the considered fcc crystal/fluid interface. Apart from Spaepen's analysis, that supports extremely large amounts of undercooling never obtained on transition metals, there is a good agreement between the experimental results, including Turnbull's initial result, and the most recent simulations on α_{LS} or θ.

III. LIQUID-VAPOUR SURFACE ENERGIES

The data relative to non refractory elements come from Keene's review (43) and are mean values calculated from all the available data for σ_{LV}, mainly obtained by using the sessile drop and maximum bubble pressure techniques. However, a suitable way to measure the liquid-vapour surface energy σ_{LV} for reactive and high melting point materials is the drop weight technique practiced at the extremity of a

pendant wire with an electron bombardment heating. The liquid-vapour surface energy is deduced by applying a modified form of Tate's law

$$mg^\circ = 2\pi r_W \sigma_{LV} F \ , \qquad [7]$$

where m is the mass of the collected drop, g° is the acceleration due to gravity, r_W is the radius of the wire at the melting temperature and F is a tabulated empirical factor. Our work in this field relies on a careful implementation of the pendant drop technique at the top of the 48-metres high Grenoble drop-tube working under ultrahigh vacuum conditions ($\approx 10^{-9}$ mbar). Owing to uncustomary reproducibility of both the masses ($\approx 0.6\%$) and the initial temperatures (a few K) of the falling samples, propitious conditions were found to realize new liquid-vapour surface energy measurements for ten refractory metals, namely W, Re, Ta, Ir, Nb, Zr, Hf, V, Ti and Pt (44,45). In the course of these experiments, some insight into the physics of the detachment problem of pendant volumes was gained, leading to the conclusion that the discrepancies between the published values for the liquid-vapour surface energy of refractory metals was due to the complex behaviour of entrapped gases in the molten volume (44). As a matter of fact, identical experimental values ($\Delta\sigma_{LV} < \pm 0.010$ J.m^{-2}) were found when comparing our measurements with data obtained by authors using indisputably gas free specimens, *i.e.* zone melted rods.

A word of discussion on Allen's work (27) is relevant at this point. The higher experimental values are often preferred on the argument that they are closest to the true value for totally pure metal. Indeed, Allen proposed for Re a σ_{LV} value of 2.750 J.m^{-2} instead of 2.520 J.m^{-2} through our measurements. However, Allen's data are a mixing of measurements realized by both drop-weight and pendant drop methods. In this last method, σ_{LV} is deduced from a best fit procedure on pictures of the pendant profile. The application of the pendant drop method requires an accurate knowledge of the liquid density since σ_{LV} is directly proportional to ρ_{Liq}. In fact, from a methodological point of view, the pendant drop method could be useful to measure the liquid density, as rightly recognized by Ivaschenko and Martsenyuk (46). As a matter of fact, liquid densities measured by these authors for V and Nb are in excellent agreement with those obtained later by using the isobaric expansion technique. In this context, one has to remember that the liquid densities considered by Allen were calculated from room-temperature specific volumes increased for cubical expansion to the melting point and an estimated amount for fusion. Systematically overestimated values were calculated for ρ_{Liq}, *e.g.* 17.5 g.cm^{-3} for W instead of 16.2 g.cm^{-3} through measurements performed later. Another weakness of Allen's work is that his data for the drop-weight method are deduced from an extrapolation procedure at zero rod diameter depending on the melting temperature, which has obviously no physical basis. Nonetheless, Allen's experimental results in terms of drop shape factors can be reinterpreted. In the lack of a new measurement on σ_{LV} for Os, it is possible to consider the value obtained from the drop-weight method (2.400 J.m^{-2}, instead of 2.500 J.m^{-2} through the pendant drop-technique) and to correct the liquid density (from 20.1 x 10^3 kg.m^{-3} down to 19.2 x 10^3 kg.m^{-3}). Concerning Ru, in connection with a liquid density of 10.7 x 10^3 kg.m^{-3} (47), Rh (48) and Mo (49), other values available in the literature have been selected that are a few percentage points below Allen's original proposals. According to Skapski (50), the variation of liquid-vapour surface energy of molten metals at melting temperature is often plotted as :

$$\sigma_{LV} = C \frac{\Delta H^\circ_{vap}}{V_m^{2/3}} \qquad \Rightarrow \qquad \alpha_{LV} = \frac{(N V_m^2)^{1/3}}{\Delta H^\circ_{vap}} \sigma_{LV} \qquad [8ab]$$

where ΔH_{vap}° is the heat of vaporisation at zero temperature. However, by analogy with Eq. [6b], C multiplied by $N^{1/3}$ can be considered as a dimensionless surface energy α_{LV} and so, potentially, as an intrinsic property of the metal under consideration. To apply the above equations, it is possible to consider for the liquid densities of refractory metals the scarce measurements realized using: (*i*) an isobaric expansion technique (Ti, V (51), Ta, W (52), Nb (53), Ir (54), Re (55), Mo(56)), (*ii*) the pendant drop technique (Rh (57), Hf (58), Os and Ru in this contribution from original Allen's work) and very recently (*iii*) a high-temperature electrostatic levitator (Zr (59)). The other data come from Smithells Metals Reference Book (60). Concerning the molar mass, melting temperature and heat of vaporization, we have considered the recent critical analysis realized by Dellacherie and Solimando (61). For the elements not considered by these authors (V, Nb, Hf, Rh, Ta, Ir, Ru and Tc) we have taken into account the values reported by the University of Sheffield (62) for ΔH_{vap}°.

IV. SOLID-LIQUID INTERFACE ENERGIES

IV.1. Undercooling results on refractory transition metals

Literature surveys of nucleation experiments have been realized by Hofmeister (65) and Cortella (66) as introductive parts of their work on refractory metals studied by drop-tube processing. Undercooling experiments on tiny refractory droplets (W, Mo and Ta) have been performed by Nelson (67) and by Rinderer et al (68,69) from *exploded* wires. If this method, on the verge of atomisation techniques, could allow large amounts of undercooling, temperature measurement on droplets collections can hardly be considered reliable enough. Temperature measurement in high drop-tube facilities has extensively been discussed elsewhere (70,71). During the free-fall, the brightness of the single droplet is tracked by a series of high-speed silicon diodes. The recording of the recalescence event offers two independent ways to determine the nucleation temperature T_n. Measuring the duration of radiant cooling from release to nucleation event, T_n may be first calculated via a numerical integration of the cooling rate which takes into account linear evolutions of liquid density (29), heat capacity (72) and hemispherical emissivity. Considering only data at the melting temperature leads to an overestimation of ΔT, as made on Nb by Lacy *et al* (73) in their pioneer work in this field (*i.e.* 530 K instead of 450 K). Moreover, the initial temperature can be identified with T_m only for indisputably gas-free specimens. Otherwise a significant increase of droplet temperature appears prior to release due to the harmful action of the entrapped gases. This leads to an increase of the cooling time to reach T_n and so an overestimation of undercooling (71). Alternatively T_n can be determined by single color pyrometry from the height of the recalescence peak assuming that the post-recalescence temperature identifies with the melting temperature of the metal (70).

From a practical point of view, the differences in undercooling determinations of W, Ta, Nb and Ir through these two methods are smaller than the combined uncertainty of either approach. The largest undercooling amount of 350 K recently reported for Zr by Morton *et al* (25) using an electrostatic levitator with direct optical pyrometry for temperature measurement, is equivalent to this obtained in our facility on this metal. The sole exception is found for Re that reaches the hypercooling regime (15), *i.e.* the post-recalescence temperature does not reach T_m. So, a great confidence has been gained in the used thermophysical properties (mainly coming from isobaric expansion technique for ρ, ΔH_m and C_P) and consequently on undercooling amounts. This data base has fruitfully been tested to interpret the numerous metastable phenomena observed in the course of our drop-tube experiments, in particular the experimental evidence of transitory metastable phases for Ta and Re coupled with a theoretical approach from first-principles calculations for identification (74).

A non satisfactory situation nevertheless remains in the case of Mo where the problem of entrapped gases is difficult to solve explaining a limited number of successful experiments. This metal has been presented (23,24) as showing the lowest undercoolability ($\theta \approx 0.10$) on the basis of thermophysical measurements realized by Seydel *et al* (75) and leading to abnormal high ΔH_m (48430 $J.mol^{-1}$) and C_P (47.95 $J.mol^{-1}.K^{-1}$). On the simple idea that sintered wires were employed in these experiments, we have considered the data from Hultgren *et al* (76), *i.e.* 27830 $J.mol^{-1}$ for ΔH_m and 34.25 $J.mol^{-1}.K^{-1}$ for C_P, already used by Hofmeister (65). Applying these data to Cortella's original result (66) (*i.e.* a free-fall time of 1.538 s to recalescence for a droplet mass of 0.251 g) leads to $\theta \approx 0.18$. Concerning Hf and Pt, the θ values given in Table 1 come from new experiments. The value for Rh is due to Hofmeister (65). Due to the lack of wires to apply the pendant drop technique in high drop-tube facilities, no undercooling experiments have been realized so far on Os and Ru. No data are also available for Tc (obviously), Cr and V.

IV.2. Undercooling results on other elements

The undercooling experiments on non transition elements have mainly been performed using emulsion or dispersion techniques. The values considered in Table 1 come from the literature survey due to Perepezko (11) who has realized numerous investigations on low melting point elements (30). The non refractory transition elements (Cu, Ag, Au, Cr, Mn, Fe, Co, Ni, Pd, Cd and Hg) have been studied by means of crucible, electromagnetic levitation, emulsion or dispersion techniques. As shown in Table 2, there is a good agreement between the values obtained by these techniques for Pd, Cu, Ag and Au, especially if we remember that an increase of ΔT is expected through the use of smaller

samples (*i.e.* the effect of K_V* shown in Fig.1). Concerning Ni, Hofmeister (65) rightly pointed out that the result obtained by Gomersall *et al* (13) should be viewed with caution until the experiment can be repeated. As a matter of fact, Willnecker *et al* (77) were only able to confirm a modest undercooling in spite of the use of an ultrahigh vacuum system. Nevertheless, contemporary to this last work, one does have to take into consideration the experiment performed by Schade *et al* (78) that confirms Gomersall's investigation. Both Shade's and Gomersall's results are in good agreement with the value reported by Ovsienko *et al* (79) by dispersion technique. An identical situation is found for Fe with two experimentally proposed values around $\theta \approx 0.17$ (9,77) and $\theta \approx 0.29$ again (78,80). In the case of Co the undercooling amounts obtained by the dispersion technique (10,79) appear significantly higher to those established by the levitation technique, including Schade's contribution (78). If the largest amount is here taken into consideration by analogy with Fe and Ni, our purpose is also to identify key experiments that could remain on pure elements. Finally, the undercoolability of Zn is derived from the value of σ_{LS} coming from dihedral angle measurements (81).

	Crucible	ref	Cont.-less	ref	Disp. Techn.	ref	Selected
Mn					0.206	(9)	0.190
Pd	0.170	(83)			0.182	(9)	0.170
Ag	0.203	(84)			0.205	(21)	0.200
Cu	0.161	(85)	0.196	(86)	0.204	(21)	0.190
Au	0.142	(83)			0.172	(9)	0.160
Ni	0.168	(83)	0.278	(78)	0.272	(79)	0.270
					0.203	(10)	
Co	0.175	(83)	0.198	(78)	0.272	(79)	0.260
					0.238	(10)	
Fe	0.155	(83)	0.297	(78)	0.304	(80)	0.290
			0.179	(77)	0.164	(9)	

Tab.2: Maximum normalized amounts of undercooling obtained on non refractory transition metals by crucible, container-less processing (electromagnetic levitation) and emulsion or dispersion techniques (note: since the undercooling experiments on refractory metals have been exclusively realized by container-less processing, the undercooling obtained by the dispersion technique has been slightly lowered to take into account the K_v* effect).

V. CORRELATIONS WITH THE POSITION IN THE PERIODIC TABLE

V.1. Liquid-vapour surface energies, solid-liquid interface energies

Fig. 3a shows the variation of σ_{LV} at the melting point for the *3d*-, *4d*- and *5d*- transition metals. The general trends given by Allen (27) remain, including the presently added Zn, Cd and Hg transition elements, in spite of significant modifications towards lower values of data through new measurements. However, Allen points out that the estimated surface energy of Mn and Tc are less than those of neighbouring metals. If this point is confirmed for Mn, this is not the case for Tc for which the estimation at 2.100 $J.m^{-2}$ (63) now appears compatible with the maximum for the *4d*- series. By reference to Re (or Tc), the difference in liquid-vapour surface energies is higher for Hg (or Cd) than for Hf (or Zr). The solid-liquid interface energies σ_{LS} are determined from undercooling experiments by applying Eq. [5ab]. It is assumed that the maximum amounts of liquid undercooling reported in the literature, especially for non refractory metals, are consistent with homogeneous nucleation. As shown in Fig.3b, a first remarkable result is that the solid-liquid interface energies of transition metals follow the same trends as that the liquid-vapour surface energies with respect to the position in the periodic table. In the case of the *4d*-series, the behaviour is clear enough to propose a σ_{LS} value for Tc and consequently an estimated amount of undercooling of $\theta \approx 0.24$ very close to that of Re. Concerning the *3d*-series, Mn shows the same anomaly as for σ_{LV}, suggesting an identical behaviour for the other elements. In particular, giving V and Cr the same σ_{LS} value as that of Ti or Mn would give an unacceptably low normalized undercooling of $\theta \approx 0.08$. Assuming the same trend on both σ_{LV} and σ_{LS} from Ti to Mn nevertheless leads to modest undercooling for V ($\theta \approx 0.15$) and Cr ($\theta \approx 0.13$). When

assuming the reliability of the largest results obtained on Fe and Ni, a quite identical undercoolability can be expected for Co since another anomaly would be difficult to understand in this series.

Fig.3c shows the corresponding trends for the dimensionless α_{LV}. It has been pointed out (43,64) that there is a good correlation with Eq. [8a] taking into account a slope C of 0.16×10^{-8} (*i.e.* $\alpha_{LV} \approx 0.135$). However the tendencies found through groups or periods indicate that this correlation is somewhat simplistic (also for non transition elements). Among the transition metals, Zn, Cd and Hg exhibit high dimensionless interface energies essentially through low $\Delta H_{vap}°$ values. The translation of the trends obtained on σ_{LS} in terms of dimensionless interface energy α_{LS} (Fig.3d) leads to find the majority of transition metals between 0.40 and 0.50, so around the classical Turnbull value of 0.45, *i.e.* 0.482 ± 0.060 ($\approx \pm 12\%$) on all transition metals. The mean dimensionless solid-liquid interface energies obtained on elements having the same crystallographic structure increase with the following sequence A4 (cubic, diamond type), A2 (cubic, W type), A1 (f.c.c., Cu type) and A3 (h.c.p., Mg type) as shown in Table 3. Note that the average values obtained for the compact f.c.c. and h.c.p. structures are in excellent agreement with the recent calculation from molecular dynamics of Davidchack and Laird (42), *i.e.* 0.51. However, these mean values can not be used to predict particular behaviours, since the most concrete physical meaning is found through the corresponding dimensional energies. This last point of view is particularly well exemplified for Hg which otherwise could appear as an exception.

Structure	Elements	α_{LS}	Δ (%)
A4	Ge, Si	0.400	0.5
bcc (A2)	Cr, W, V, Nb, Mo, Ta	0.427	8.6
bcc ► hcp	Ti, Zr, Hf	0.468	1.5
fcc (A1)	Pt, Pd, Cu, Ni, Ir, Rh, Au, Ag, Pd	0.484	12.0
hcp (A3)	Cd, Zn, Ru, Os, Tc, Re	0.501	8.6
others	In (A6), Ga (A11), Hg (A10)	0.648	5

Tab.3: Mean dimensionless solid-liquid interface energy versus crystallographic structure (A4: cubic, diamond type, A6: tetragonal, A10: rhombohedral, A11: orthorhombic).

V.2. Critical nucleus and dimensionless β number

On the basis of the above consideration, trends for the critical nucleus size cannot evidently be supposed. At least, r* could appear as:

$$r^* = 2\frac{\alpha_{LS}}{\theta}\left(\frac{V_m}{N}\right)^{1/3}, \qquad [9]$$

so the product of α_{LS}/θ by an intrinsic length L that reflects compactness through $V_m^{1/3}$. As shown in Fig.4a this length displays a parabolic behaviour in each series with the sole anomaly of Mn. This behaviour is the consequence of the liquid density ρ_{Liq} variation versus atomic number that is also found for the solid at ambient temperature (Fig.4b). This explains why L focuses attention on elements placed on the *right side* of each series, as for instance Ir for the *5d*-series. The trends of the critical nucleus size r* are well defined for *4d*- and *5d*- transition metals and more clear than those obtained for α_{LS} (Fig.4c).

Following Skapski, the ratio of σ_{LS} to σ_{LV} leads to introduce a dimensionless β number. This number has been often considered roughly constant and a possible average value obtained for transition elements is 0.140 ± 0.027 (*i.e.* $\approx \pm 19\%$). Nevertheless, more subtle behaviours can be found when considering this number (Fig.4d). As a matter of fact, the anomaly of Mn disappears in the *3d*-series while the other elements follows a regular increase to Ni. For the *4d*-series the parabolic form is resumed but for the Tc value which is slightly lower than the values obtained for Mo and Ru placed on each side in the series. It is noteworthy that an anomaly appears for Ag that show a highest β value than this suggested by the trend. A decrease in β can be obtained through a significant decrease of σ_{LS} which is unlikely or an increase of σ_{LV} which could appear more satisfactory with the trend observed for σ_{LV} through the *4d*-series (Fig.3a). Finally, the *5d*-series displays a parabolic shape with again a maximum for W. Moreover, β is found to follow a remarkable linear dependency against the melting temperature

with a confidence interval of 98.3% which is only obtained for this series (Fig.5a). This interval is only of 92% when considering independently the evolutions of σ_{LV} and σ_{LS} against the melting temperature.

Taking into account the limited number of elements for each period when discussing the non transition elements, it is difficult enough to find trends for both σ_{LV} and σ_{LS} values. As for the transition metals, the use of the dimensionless energies do not allow any clarification. Nonetheless, a clear classification of behaviours into several groups, namely metals, semimetals, semiconductors and the somewhat exotic Se and Te elements appears by using the dimensionless β number (Fig.5b). The metals are characterized by a β value of the same order as that obtained for transition elements. Nevertheless, it must be noticed that the *apparently* good agreement for Al is obtained using a liquid-vapour surface energy of 0.870 $J.m^{-2}$. However, as pointed out by Keene (43), several measurements suggest that most data for σ_{LV} of Al pertain to oxygen saturated material and that for pure metal σ_{LV} could be of the order of 1.075 $J.m^{-2}$. Assuming the same β value leads to a solid-liquid interface energy of 0.132 $J.m^{-2}$, so to expect a highest amount of undercooling for this element (25 % of T_m instead of 17 %).

V.3. Other physical properties

The behaviours displayed by σ_{LS} and σ_{LV} are fruitfully compared to those of cohesion energies of solids E_c (Fig.4c) and melting temperatures T_m (Fig.4d) through these series (82). A similar parabolic trend is found for both E_c and T_m values of the *5d*-series. A good resemblance between E_c, T_m, σ_{LV} and σ_{LS} curves is encountered for the *3d*-series with the Mn anomaly and a relative plateau for the Fe, Co, Ni. The *4d*- series is mainly characterized by a strong anomaly for the manmade element Tc. If the data reported by Iida and Guthrie (87) do not suggest any correlation for the boiling temperatures T_b, this is not the case (Fig. 6a) taking into account the recent review proposed by Dellacherie and Solimendo (61).

The experimental data on the liquid-vapour surface energy or liquid density at the melting temperature are accurate enough to give clear correlations. This is generally not the case when considering the coefficients in temperature, leading to find some support from models. Calculations of $d\sigma_{LV}/dT$ have been originally performed using the Eötvös' law (*see* Ref. 87). Based on two different physical approaches, Miedema and Boom (88) and more recently Eustathopoulos *et al* (89) were led to propose the same following expression for $d\sigma_{LV}/dT$ (or σ'),

$$\sigma' = -\frac{b}{N^{1/3}V_m^{2/3}} + \frac{2}{3}\frac{\sigma}{\rho_{Liq}}\frac{d\rho_{Liq}}{dT} \qquad \sigma' = -\frac{2}{3}\frac{\sigma}{\rho_{Liq}}\left[\frac{\rho_{Liq}S_S}{fN^{1/3}\sigma V_m^{1/3}} - \frac{d\rho_{Liq}}{dT}\right] \qquad [10ab]$$

where in Eq. [10a], b identifies with an entropy. This entropy is determined from experimental σ' data in Ref. 88, leading to a mean value of 4,14 $J.mole^{-1}.K^{-1}$. In the work of Eustathopoulos *et al* (89), b is defined by applying Skapski's model (26,90) as the ratio S_S/f, where S_S is the surface entropy and f is a factor of compactness (Eq.10b). Assuming the three modes of oscillation of a surface atom equivalent and the surface structure of liquid metals well approximated by the plane (111) of f.c.c. metals, b is equal to 4,86 $J.mole^{-1}.K^{-1}$ with $S_S = 5.3$ $J.mol^{-1}.K^{-1}$ and $f = 1.091$. The prediction of this model mainly depends on the experimental data on $d\rho_{Liq}/dT$, that seems only well determined for the *3d*-series, assuming that this property should be connected with the atomic number (Fig.6b). The calculated values range between – 0.15 $mJ.m^{-2}.K^{-1}$ for Cd or Hg to – 0.35 $mJ.m^{-2}.K^{-1}$ for Cr (Fig.6c), that is of the same order of the experimental spread on σ' for Cu. We may believe that the value reported for Zr by Paradis and Rhim (59) for $d\sigma_{LV}/dT$ (-0.24 $mJ.m^{-2}.K^{-1}$) is probably more reliable than the abnormal low value obtained for $d\rho_{Liq}/dT$ (-0.29 $kg.m^{-3}.K^{-1}$) during the same experiments by electrostatic levitation. The critical temperature T_c, for which the liquid-vapour surface energy drops to zero, can be estimated by applying Eötvös' law (*see* Ref. 87).

As a last remark, a simple relation between liquid-vapour surface energy and viscosity η (Eq. [11]) has been deduced by Egry (91) from statistical mechanics,

$$\eta = \frac{\sigma_{LV}}{0.86}\sqrt{M/RT_m} \qquad , \qquad [11]$$

with a good agreement with experimental data. This relation, leading to the correlations given in Fig.6d, is of a great interest since its links a surface property σ_{LV} to a bulk property η and consequently to bulk diffusion via the Stokes-Einstein relation (*see* Ref. 87).

VI. CONCLUSION

Numerous physical properties are closely related to the position of the element in the periodic table. Evidences in such correlations are particularly gained when focusing attention on the elements of *4d*- and *5d*-series. However, experience is often difficult to be realized, since these key-elements display a refractory character. In this context, it is not surprizing that drop-tube experiment on such metals has led to the possibility to discuss the level of undercooling of a very large number of elements, and to our knowledge this is the first tentative in individualizing each behaviour. The most interesting result was in establishing that the solid-liquid interface energy determined from undercooling experiments can be also connected to the position of the element under consideration in the periodic table. As a matter of fact, no significant unexplained anomaly has been identified making believe that the classical theory furnishes a robust support to describe the crystal nucleation. The *5d*-series, that do not present any physical anomaly, shows the most perfect parabolic trends for dimensional properties such as energy of cohesion, melting temperature, density, liquid-vapour surface energy, solid-liquid interface energy. In spite of clear correspondences with the crystallographic structure, the use of the dimensionless solid-liquid interface energy α_{LS} appears of little interest since the most concrete physical meaning is found through the dimensional energy. A classification of the elements into different groups is obtained by considering the β number, the main division being between metals and non metals.

The correlations found in the course of this work for the solid-liquid interface energy are clear enough to be thought to have a physical consistency, so that the maximum amounts of undercooling reported in the literature should be consistent with homogeneous nucleation. This is an encouraging result for a better description of heterogeneous nucleation, but also to develop an experimental strategy for studying alloys. It remains that homogeneous nucleation can only be claimed on the basis of kinetics measurements, but not on the simple argumentation of reaching a temperature fitting well with the trends. These kinetics measurements are also of a central importance when dealing with alloys, due to the possibility in getting significant variations of K_v, as theoretically established for instance in the case of multicomponent liquid alloys (92). Concerning pure metals, it is not in doubt that several experiments remain to be undertaken as for instance of V for a more complete overview. Moreover, the situation for the Fe, Co and Ni triad can not be said satisfactorily enough in comparing their undercoolability. In case of choice, the undercooling experiments should be focused on Co. Finally, the application of container-less processing is expected to allow a better knowledge on refractory transition metals and alloys (93), that are gaining increasing importance in the high technology field.

ACKNOWLEDGEMENTS

The contribution of BV is realized within an agreement between CEA and CNES. It is also part of ESA - Microgravity Application Programs entitled “High-Precision Thermophysical Property Data of Liquid Metals for Modelling of Industrial Solidification Processes” (coordinated by Hans Fecht, University of Ulm) and “Study and Modelling of Nucleation and Phase Selection Phenomena in Undercooled Metallic Melts” (coordinated by Wolfgang Löser, IFW-Dresden and BV). LM is thankful for the financing from A. Hultqvists Fond and Rymdstyrelsen. Thanks are due to Béatrice Drevet, Jean-Paul Garandet and László Gránásy (ISSPO, Budapest) for fruitful comments.

REFERENCES

1. Eustathopoulos, N., *Int. Met. Rev.* **28**, 189 (1983).
2. Fahrenheit, D.B., *Phil. Trans. Royal Soc. of London* **39**, 78 (1724).
3. Berthollet, C. L., *in* « Essai de Statique chimique » **1**, 32 (1803).
4. Larousse, P., *in* « Grand Dictionnaire du XIX siècle » **14**, 1230 (1866).
5. Gernez, M.D., *Comptes Rendus de l’Académie des Sciences* **60**, 833 (1865).
6. Van Riemsdyk, A. D., *Annales de Chimie Physique* **20**, 66 (1880).
7. Mendenhall, C.E., and Ingersoll, L.R., *Phil.Mag.* **15**, 205 (1908).

8. Vonnegut, B., *J. of Coll. Sci.* **3**, 563 (1948).
9. Turnbull, D., and Cech, R.E., *J. of. Appl. Phys.* **21**, 804 (1950).
10. Rasmussen, D.H., Javed, K., Appleby, M., and Witomski, R., *Mat. Lett.* **3**, 344 (1985).
11. Perepezko, J.H, *Mater. Sci. Eng. A* **65**, 125 (1984).
12. Bosio, P.L., Cortes, R., and Defrain, A., *J. de Chimie Physique* **70**, 357 (1973).
13. Gomersall, D.W., Shiraishi, S.Y., and Ward, R.G., *J. of Aust. Inst. Met.***10**, 220 (1965).
14. Hofmeister, W.H., Robinson M.B., and Bayuzick, R.J., *Appl. Phys. Lett.* **49**, 1342 (1986).
15. Vinet, B., Cortella, L., Favier J.J., and Desré, P.J., *Appl. Phys. Lett.* **58**, 97 (1991).
16. *in* "The Collected Works of J.W. Gibbs", Ed.. by Longman-Green, New-York **vol 1**, 55 (1932).
17. Volmer, M., and Weber, A., *Zeit. Für Phys. Chemie* **119**, 277 (1926).
18. Becker, R., and Döring, W., *Annalen der Physik und Chemie* **25**, 719 (1935).
19. Turnbull, D., and Fisher, J.C., *J. of Chem. Phys.* **17**, 1 (1949).
20. Turnbull, D., *J. of Appl. Phys*. **17**, 71 (1949).
21. Skripov, V.P., *in* "Crystal Growth and Materials" (E. Kaldis and H.J. Scheel, Eds.), p.328. North-Holland, Amsterdam, 1977.
22. Turnbull, D., *J. of. Chem. Phys.* **20**, 411 (1952).
23. Vinet, B., *Int. J. of Thermophysics* **20**, 1061 (1999).
24. Cortella, L., and Vinet, B., *Phil. Mag.B* **71**, 11 (1995).
25. Morton, C. W., Hofmeister, W. H., Bayuzick, R. J., Rulison, A. J., and Watkins, J. L., *Acta Mater*. **46**, 6033 (1998).
26. Skapski, A.S., *Acta. Metall.* **4**, 576 (1956).
27. Allen, B.C., *Trans. Met. Soc. of AIME* **227**, 1175 (1963).
28. Turnbull, D., *J. of Appl. Phys*. **21**, 1022 (1952).
29. Perepezko, J.H., and Paik, J.S., *in* "Rapid Solidified Amorphous and Crystalline Alloys" (B.H. Kear, B.G. Giessen and M. Cohen, Eds), p.49. Elsevier Science, New-York, 1982.
30. Rasmussen, R., Perepezko, J.H., and Loper Jr., C.R., *in* "Second International Conference on Rapidly Quenched Metals" (N.J. Grant and B.C. Giessen, Eds.), p.51. Massachusetts Institute of Technology Press, Cambridge, vol 1, 1976.
31. Koverda, V.P., Skokov, V.N. and Skripov, V.P., *Physica Status Solidi* **A74**, 343 (1982).
32. Zeldovich, Ya.B., *Zurnal Eksperimentalnoj i Teoreticeskoj Fiziki* **12**, 525 (1942).
33. Howe, J.M., *in* "Interfaces in Materials" p.219. John Wiley & Sons, Inc, New-York, 1997.
34. Gránásy, L., *Int. J. of Non-Equil.Process*. **11**, 113 (1998).
35. Spaepen, F., *Acta Metall.* **23**, 14 (1975).
36. Spaepen, F., and Mayer, R.B., *Scr. Metall.* **10**, 257 (1976).
37. Thompson, C.V., Ph-D Thesis, Harvard University 1981.
38. Howe, J.M., Dahmen, U., and Gronsky, R., *Phil. Mag.A* **56**, 31 (1987).
39. Broughton, J.Q., and Gilmer, G.H., *J. of Chem. Phys*. **84**, 5749 (1986).
40. Iwamatsu, M., *J. Phys.: Condens. Matter* **11**, L1 (1999).
41. Iwamatsu, M., *Mat. Sci. Forum* **343/346**, 9 (2000).
42. Davidchack, R.L., and Laird, B.B., *Phys. Rev. Lett.* **85**, 4751 (2000).
43. Keene, B.J., *Int. Mat. Rev.* **38**, 157 (1993).
44. Vinet, B., Garandet, J.P., and Cortella, L., *J. of Appl. Phys*. **73**, 3830 (1993).
45. Vinet, B., and Garandet, J.P., *in* "Second International Conference High Temperature Capillarity" (N. Eustathopoulos, Ed.), p.223. Reproprint, Bratislava, 1995.
46. Ivaschenko, Yu.N., and Martensyuk, P.S., *Teplofiz. Vyz. Temp.* **11**, 1285 (1973).
47. Martensyuk, P.S. and Ivaschenko, Yu.N., *Adgez. Rasp. Paika Mater.* **20**, 15 (1988).
48. Eremenko, V.N., and Naidich, Yu.V., *Izv. Akad. Nauk. SSR OTN Met. Topliva* **6**, 100 (1961).
49. Namba, S., and Isobe, T., *in* "4th Symposium on Electron Beam Technology" (R. Bakish, Ed.), p.96., 1962.
50. Skapski, A.S., *J. Chem. Phys*. **16**, 386 (1948).
51. Seydel, U., and Kitzel, W., *J. Phys. Chem. F: Metal Phys.* **9**, 153 (1979).
52. Berthault, A., Arlès, L., and Matricon, J. *Int. J. of Therm.* **7**, 167 (1986).
53. Gallop, R., Jäger H., and Pottlacher, G. *High Temp.-High Press.* **17**, 207 (1985).
54. Gathers, G.R., Shaner, J.W., Hixson, R.S., and Jung, D.A., *High Temp.-High Press.* **11**, 653 (1979).

55. Thévenin, T., Arlès, L., Boivineau, M., and Vermeulen, J.M., *Int. J. of Therm.* **14**, 441 (1993).
56. Shaner, J.W., Gathers, G.R., and Minichino, C., *High Temp.-High Press.* **9**, 331 (1977).
57. Popel, S.I., Tsareveskii, B.V., and Dzhemilev, N.K., *Fiz. Met. Metall. SSSR* **18**, 468 (1964).
58. Ivaschenko, Yu.N., and Martensyuk, P.S., *Zavod. Lab.* **39**, 42 (1973).
59. Paradis, P.F., and Rhim, W.K., *J. Mater. Res.* **14**, 3713 (1999).
60. Brandes, E.A., and Brook, G.B., *in* "Smithells Metals Reference Book", Butterworth – Heinemann, Oxford, 7th edition, 1992.
61. Dellacherie, J., and Solimando, R., *in* « Techniques de l'Ingénieur, Traité Constantes Physico-chimiques » K572, Paris, 1996.
62. University of Sheffield, www.shef.ac.uk/~chem/web-elements.
63. Siuta, V.P. and Balicki, M., WADC TR 57-241, Part II, 1957 (from ref. [26]).
64. Eustathopoulos, N., Ricci E., and Drevet, B., *in* « Techniques de l'Ingénieur, Traité Matériaux Métalliques » M67, Paris, 1999.
65. Hofmeister, W.H., Ph-D Thesis Nashville, 1987.
66. Cortella, L., Ph-D Thesis INP-Grenoble, 1993.
67. Nelson, L.S., *Nature* **210**, 410 (1965).
68. Meyer, E., and Rinderer, L., *J. of Crystal Growth* **28**, 199 (1975).
69. Houch, D., and Rinderer, L., *in* "4th Decennial International Conference on Solidification Processing" (J. Beech and H. Jones, Eds.), p.516. University of Sheffield, 1997.
70. Hofmeister, W.H., Bayuzick, R.J., and Robinson, M.B., *Int. J. of Thermophysics* **10**, 279 (1989).
71. Vinet, B., Cortella, L., and Boch, A., *Trans. Mat. Res. Soc. Jpn*. **16A**, 593 (1994).
72. Regnaut, C., and Bretonnet, J.L., *Journal de Physique* **C8**, 669 (1985).
73. Lacy, L.L., Robinson, M.B., and Rathz, T.J., *J. Cryst. Growth* **51**, 47 (1981).
74. Cortella, L., Vinet, B., Desré, P.J., Pasturel, A., Paxton, A.T., and Van Schilfgaarde, M., *Phys. Rev. Lett.* **70**, 1469 (1993).
75. Seydel, U., Bauhof, H., Fucke, W., and Wadle, H., *High Temp.-High Press.*, **11**, 635 (1979).
76. Hultgren, R., Desai, P.D., Hawkins, D.T., Gleiser, M., Kelley, K.K., and Wagman, D.D., *in* "Selected Values if the Thermodynamic Properties of the Elements", American Society for Metals, Metals Park, Ohio, 1973.
77. Willnecker, R., Herlach, D.M., and Feuerbacher, B., *Appl. Phys. Lett.* **49**, 1339 (1986).
78. Schade, J., McLean, A., and Miller, W.A., *in* "Undercooled Alloy Phases" (E.W. Colling and C.C. Koch, Eds.), p.233. Warrendale, The Metallurgical Society, 1986.
79. Ovsienko, D.E., Maslov, V.V., and Kostuchenko, V.L., *Kristallographia* **16**, 405 (1971).
80. Dukin, A.I., *in* "Problemi Metallovedenia i Fiziki Metallov" p.9. Metallurgizdat, Moscou, 1959.
81. Passerone, A., Sangiorgi, R., Eustathopoulos, N., and Desré, P.J., *Met. Sci.* **13**, 359 (1979).
82. Friedel, J., *Trans. AIME* **230**, 616 (1964).
83. Fehling, J., and Scheil, E., *Zeit. Für Metallkunde* **53**, 593 (1962).
84. Powell, G.L.F., *Trans. of the AIME* **239**, 1244 (1967).
85. Powell, G.L.F., *Trans. of the AIME*, 1969, **245**, 407.
86. Willnecker, R., Herlach, D.M., and Feuerbacher, B., *Mat. Sci. Eng.* **98**, 85 (1988).
87. Iida, T., and Guthrie, R.I.L., *in* "The Physical Properties of Liquid Metals", p.131. Oxford Science Publications, Clarendon Press-Oxford, 1993.
88. Miedema, A.R., and Boom, R., *Zeit. für Metallkunde* **69**, 183 (1978).
89. Eustathopoulos, N., Drevet, B., and Ricci, E., *J. of Crystal Growth.* **191**, 268 (1998).
90. Skapski, A.S., *J. Chem. Phys.* **16**, 386 (1948).
91. Egry, I, *Scripta Metallurgica et Materialia* **26**, 1349 (1992).
92. Desré, P.J., Cini, E. and Vinet, B., *J. of Non-Crystalline Solids* **288**, 210 (2001)
93. Vinet, B., Berne, C., Desré, P.J., Fecht, H.J., Fredriksson, H., Granasy, L., Greer, A.L., Hermann, R., Löser, W., Magnusson, L., Pasturel, A., *in* "International Symposium on Microgravity Research and Applications", p.1123, ESA – **SP454,** 2001.

	Struct	T_m K	ρ_{Liq} kg.m^{-3}	M kg.mol^{-1}	$\Delta H_{vap}°$ J.mol^{-1}	σ_{LV} J.m^{-2}	α_{LV}	ΔH_m J.mol^{-1}	θ	σ_{LS} J.m^{-2}	α_{LS}	β
Ti	hcp	1943	4110	0.0479	421000	1.525	0.157	15400	0.17	0.168	0.473	0.110
V	bcc	2175	5560	0.0509	453000	1.855	0.151	21900	0.15	0.242	0.409	0.131
Cr	bcc	2176	6280	0.0520	340200	1.642	0.167	20900	0.13	0.230	0.381	0.140
Mn	A12	1517	5730	0.0549	226100	1.152	0.194	12100	0.19	0.162	0.509	0.140
Fe	bcc	1809	7015	0.0558	349600	1.862	0.179	13800	0.29	0.269	0.656	0.144
Co	hcp	1768	7760	0.0589	376600	1.881	0.163	16200	0.26	0.289	0.581	0.153
Ni	fcc	1726	7905	0.0587	370400	1.796	0.156	17500	0.26	0.306	0.562	0.170
Cu	fcc	1356	8000	0.0636	300300	1.297	0.145	13100	0.19	0.186	0.478	0.143
Zn	hcp	693	6575	0.0653	115300	0.789	0.266	7300	0.19	0.087	0.464	0.110
Zr	hcp	2125	6240	0.0912	582000	1.435	0.124	16900	0.17	0.158	0.472	0.110
Nb	bcc	2740	7620	0.0929	683700	1.870	0.122	26900	0.16	0.262	0.435	0.140
Mo	bcc	2890	9000	0.0959	690000	2.080	0.123	27830	0.18	0.315	0.463	0.151
Tc	hcp	2430	10250	0.0989	550000	2.200	0.153	23000	0.24	0.330	0.550	0.150
Ru	hcp	2523	10690	0.1010	580000	2.180	0.142	25700	0.20	0.329	0.484	0.151
Rh	fcc	2239	10700	0.1029	495000	1.940	0.150	21700	0.20	0.279	0.492	0.144
Pd	fcc	1825	10490	0.1064	357500	1.482	0.164	17600	0.17	0.199	0.447	0.134
Ag	fcc	1234	9346	0.1079	250600	0.925	0.159	11300	0.20	0.131	0.501	0.142
Cd	hcp	594	8020	0.1124	99600	0.637	0.313	6200	0.18	0.058	0.458	0.091
Hf	hcp	2500	11970	0.1784	630000	1.545	0.125	25500	0.18	0.229	0.460	0.148
Ta	bcc	3288	14600	0.1809	735000	2.010	0.124	32020	0.19	0.335	0.473	0.167
W	bcc	3680	16200	0.1838	823900	2.310	0.120	46685	0.16	0.436	0.398	0.189
Re	hcp	3453	18000	0.1862	714800	2.520	0.141	33230	0.25	0.463	0.559	0.184
Os	hcp	3300	19200	0.1902	746100	2.400	0.125	31800	0.20	0.402	0.493	0.168
Ir	fcc	2716	20000	0.1922	560000	2.140	0.146	26140	0.19	0.322	0.471	0.151
Pt	fcc	2042	19000	0.1950	509800	1.710	0.134	19700	0.16	0.213	0.431	0.125
Au	fcc	1336	17360	0.1969	334400	1.145	0.146	12600	0.16	0.128	0.435	0.112
Hg	A10	232	13351	0.2005	59200	0.489	0.425	2300	0.38	0.031	0.686	0.063
Al	fcc	932	2385	0.0270	290800	0.871	0.127	10700	0.17	0.106	0.422	0.122
Si	A4	1685	2510	0.0280	385100	0.775	0.085	50200	0.27	0.477	0.401	0.615
Ga	A11	303	6090	0.0697	258700	0.711	0.117	5600	0.50	0.082	0.624	0.115
Ge	A4	1210	5600	0.0726	330900	0.607	0.086	36900	0.27	0.314	0.398	0.516
Se	A8	494	3989	0.0789	106600	0.103	0.059	13400	0.20	0.076	0.349	0.740
In	A6	429	7023	0.1148	231500	0.556	0.130	3300	0.26	0.037	0.611	0.067
Sn	A4	520	7000	0.1187	296100	0.562	0.105	7000	0.37	0.077	0.613	0.138
Sb	A7	903	6483	0.1217	115600	0.371	0.191	20000	0.23	0.137	0.408	0.370
Te	A8	723	5710	0.1276	104700	0.239	0.152	17900	0.33	0.127	0.473	0.531
Tl	hcp	577	11280	0.2043	164100	0.459	0.163	4100				
Pb	fcc	600	10678	0.2072	178800	0.457	0.156	4800	0.25	0.047	0.602	0.104
Bi	A7	544	10068	0.2089	138500	0.382	0.176	11300	0.42	0.099	0.560	0.260

Tab. 1: Data considered, calculated or estimated in this study (see text for references).

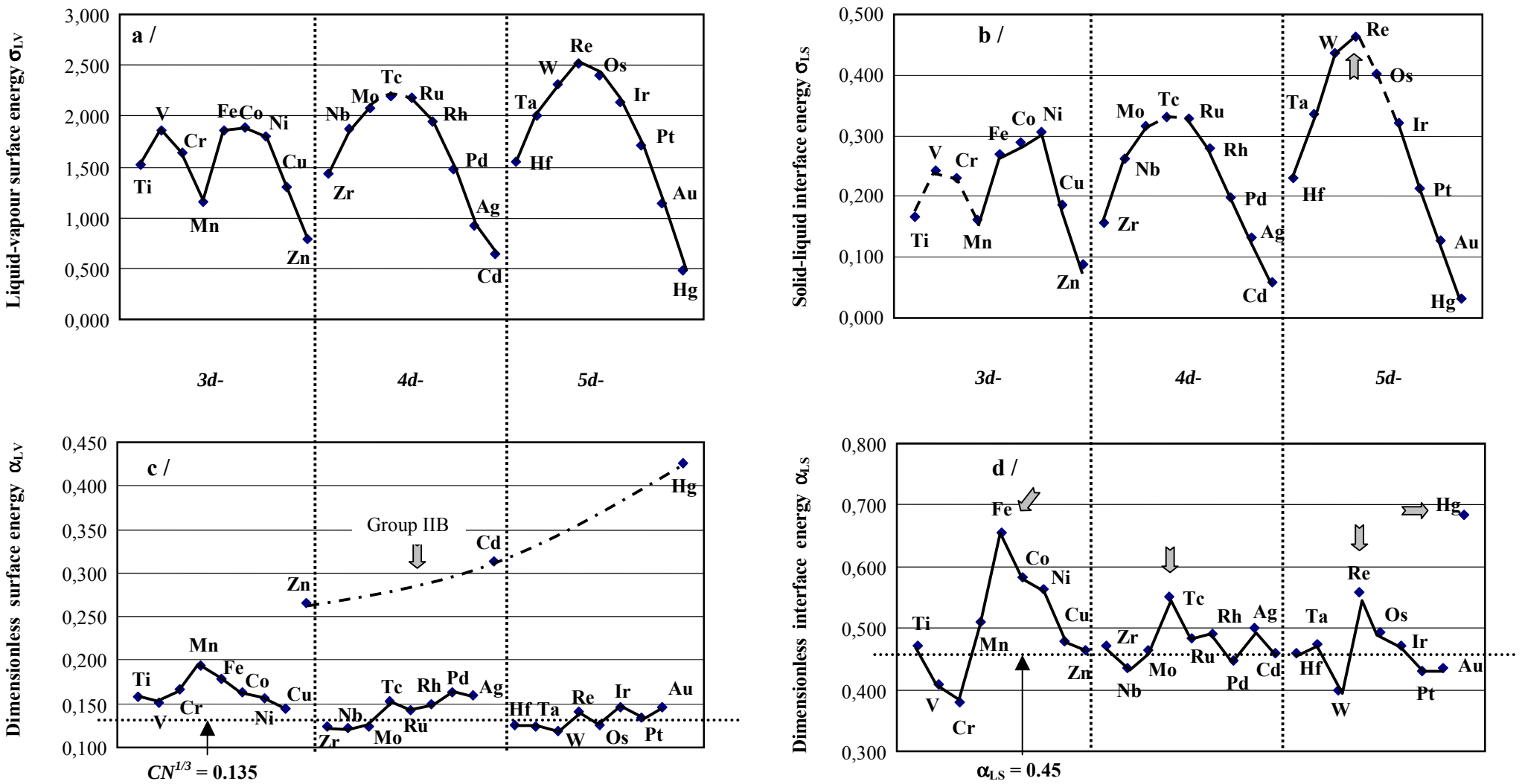

Fig. 3. a) Liquid-vapour surface energies σ_{LV}, **b)** solid-liquid interface energies σ_{LS}, **c)** dimensionless liquid-vapour surface energies α_{LV} and **d)** dimensionless solid-liquid interface energies α_{LS} for *3d*-, *4d*- and *5d*- transition metals.

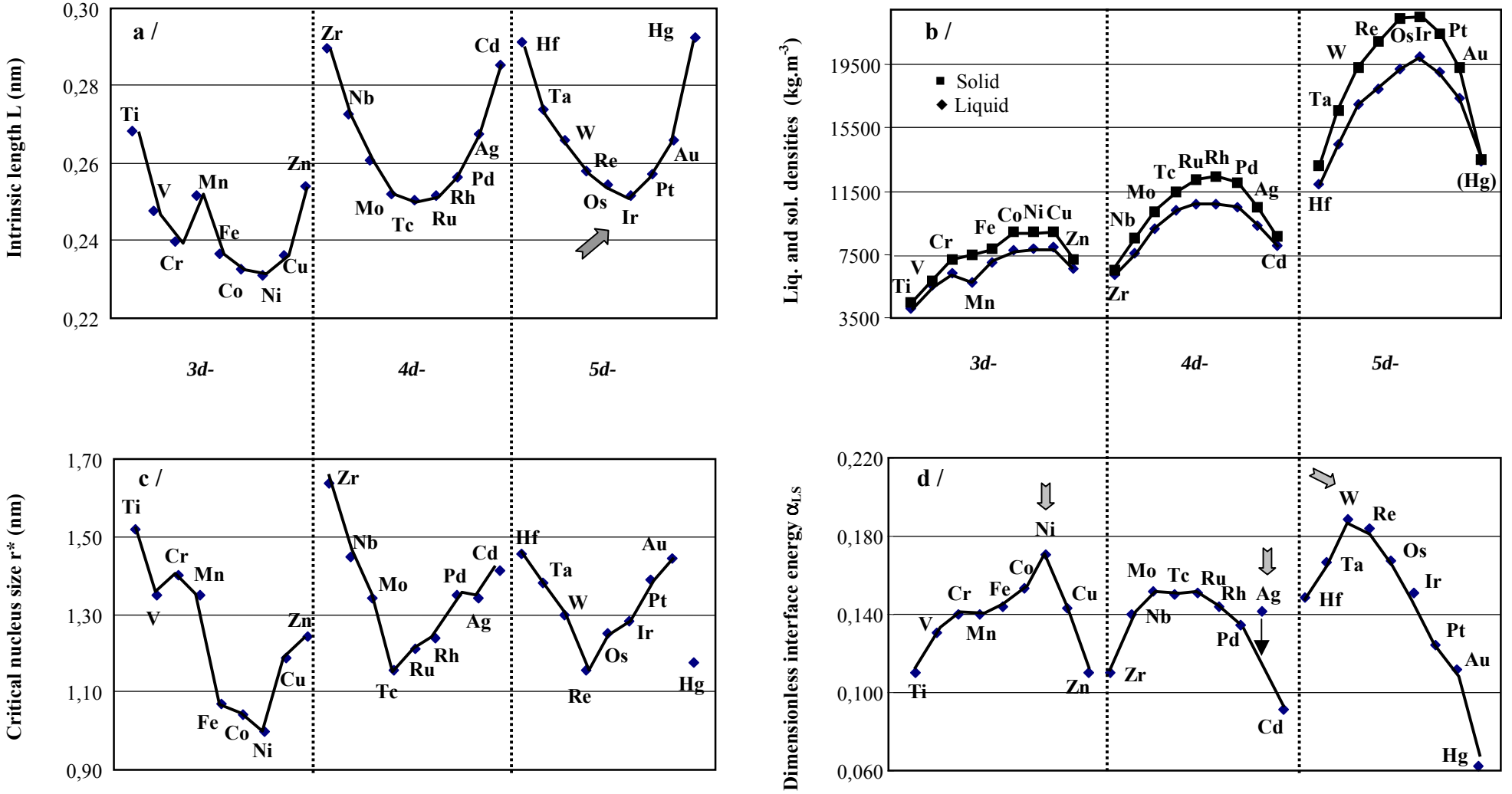

Fig. 4. a) Intrinsic length L, **b)** liquid density at T_m and solid density at ambient temperature, **c)** critical nucleus size r* and dimensionless β number for the *3d*-, *4d*- and *5d*- transition metals.

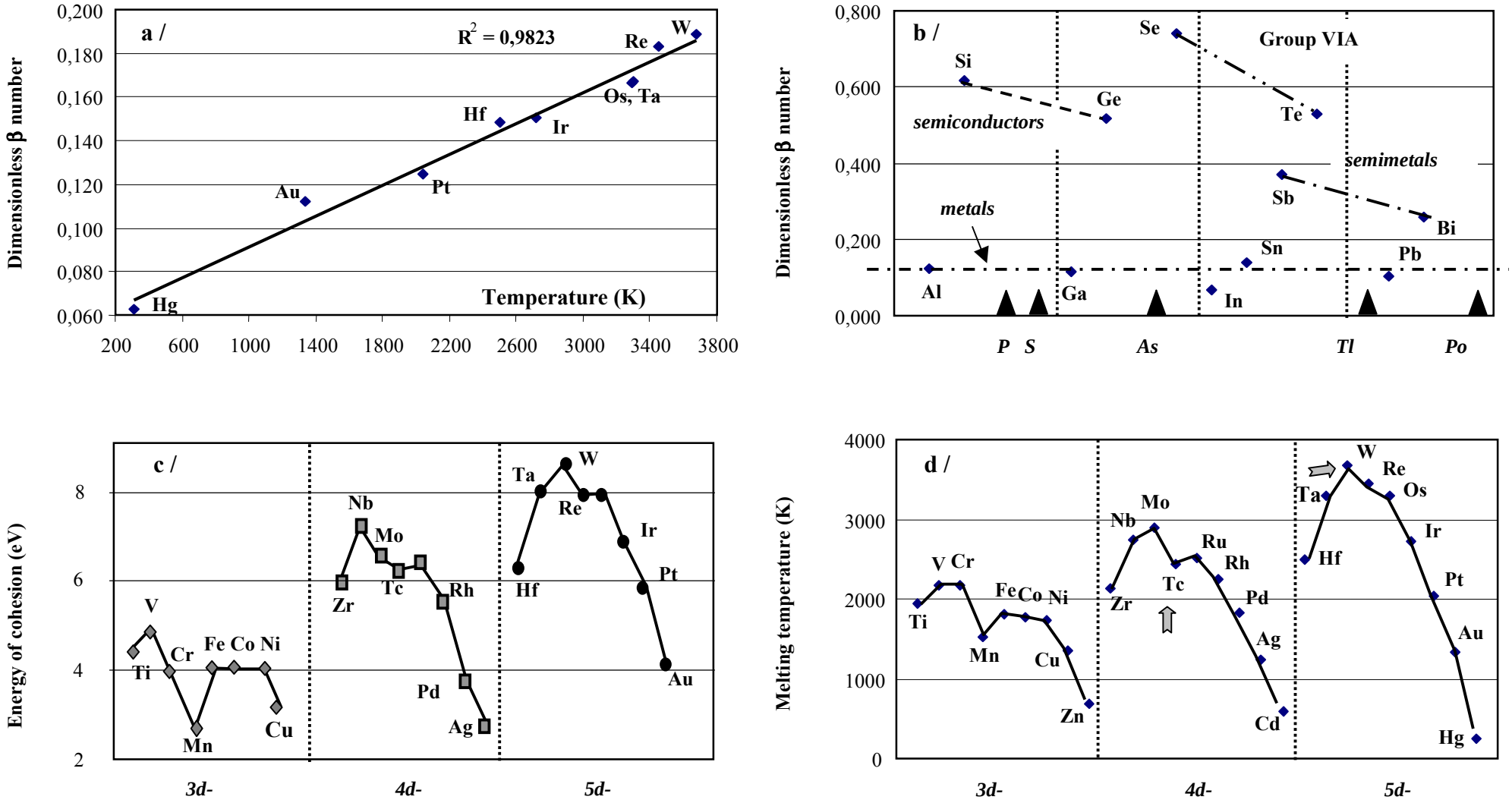

Fig. 5. a) Dimensionless β number versus melting temperature for the *5d*- elements, **b)** dimensionless β number for non transition elements (elements from both same periods and groups ▲), **c)** energy of cohesion E_c and **d)** melting temperature for *3d*-, *4d*- and *5d*- transition metals.

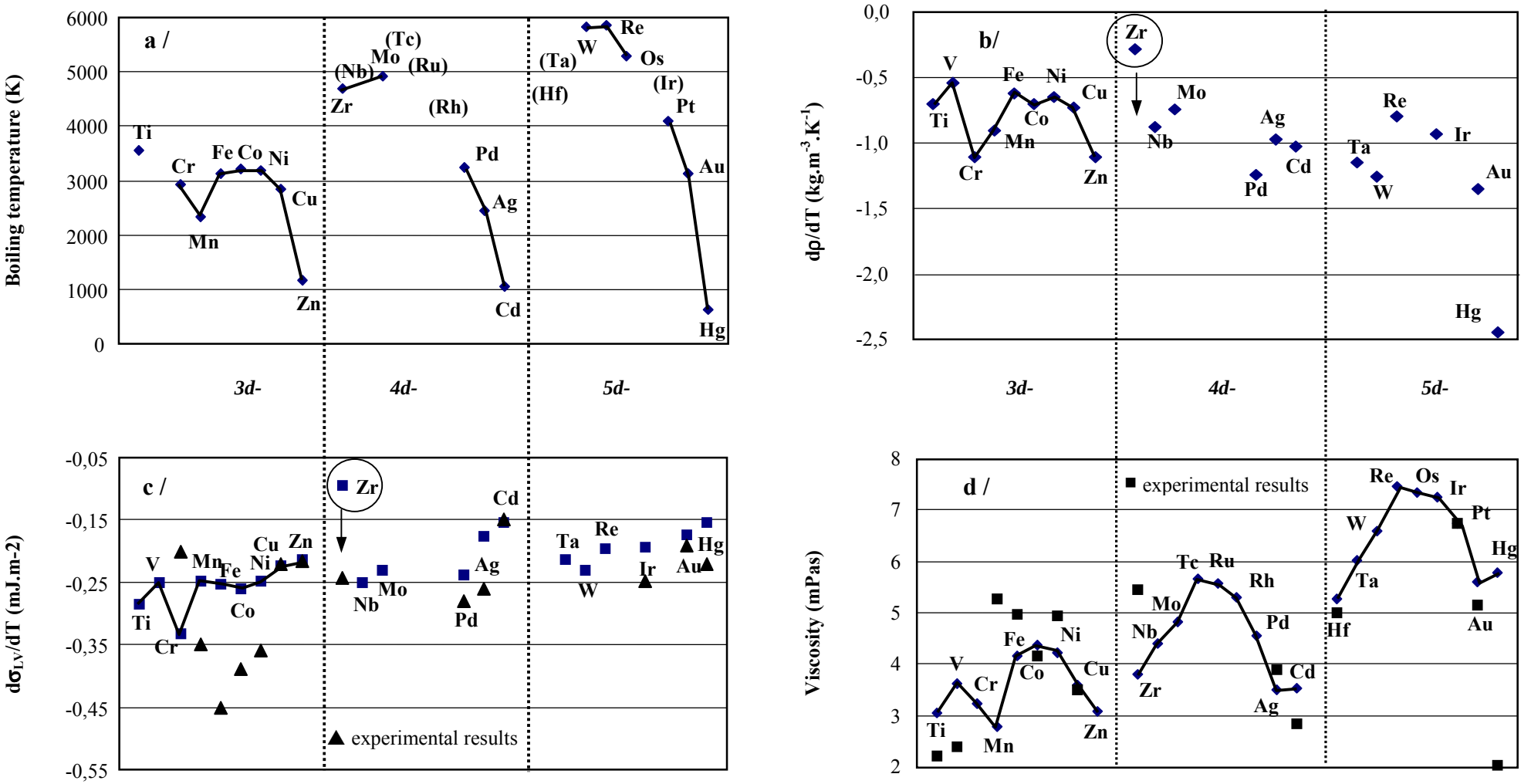

Fig. 6. a) Boiling temperature, **b)** coefficient in temperature of ρ_{Liq}, **c)** coefficient in temperature of σ_{LV} and **d)** viscosity for the *3d*-, *4d*- and *5d*- transition metals.

CRYSTAL NUCLEATION VS. CRYSTAL GROWTH The association of organic compounds with biomineralized structures (Wada and Fujinuki 1976; Crenshaw 1972; Collins et al. 1992) and their observed effect on crystallization kinetics (Sikes et al. 1990; Wheeler et al. 1990) strongly suggest that these compounds modify the growth stage of minerals. This conclusion is reinforced by observations of faceted crystal surfaces in a number of cases, including the calcite crystals shown in Figure 1d as well as numerous examples of calcium oxalate monohydrate crystals, both functionalâ€"as in plantsâ€"and pathogenicâ€"as However in crystals, the surface free energy is generally anisotropic. Consequently, the equilibrium crystal shape will not generally be spherical, but can be determined by the Gibbs-Wulff theorem. In 1878, Gibbs proposed that for the equilibrium shape of a crystal, the total surface Gibbs function of formation should be a minimum for a constant volume of crystal, i.e.: (1). where: An = area of the nth face and g n = surface tension of the nth face, which is assumed constant over the whole face and independent of the crystal shape.Â Any further increase in the pressure, say to pressure Pb , will make the gas unstable with respect to the bulk, infinitely large crystal, i.e. m v > m c, the chemical potential of the gas will be higher than that of the infinite crystal.